Adv Comput Math
DOI 10.1007/s10444-016-9461-4

Dimensions of spline spaces over non-rectangular T-meshes

Chao Zeng[1] · Meng Wu[2] · Fang Deng[1] · Jiansong Deng[1]

Received: 23 July 2015 / Accepted: 19 April 2016

Abstract Spline spaces over rectangular T-meshes have been discussed in many papers. In this paper, we consider spline spaces over non-rectangular T-meshes. The dimension formulae of spline spaces over special simply connected T-meshes have been obtained. For T-meshes with holes, we discover a new type of dimension instability. We construct a relationship between the dimension of the spline space over a T-mesh $\mathscr{T}$ with holes and the dimension of the spline space over a simply connected T-mesh associated with $\mathscr{T}$.

Keywords Spline · T-mesh · Dimension

Mathematics Subject Classification (2010) 41A15 · 65D07 · 65D17

1 Introduction

Spline spaces over T-meshes are introduced in [4]. In this paper, the dimensions of spline spaces with low-order smoothness (the smoothness order is less than half of the degree of the polynomials in the spline space) are analyzed using the B-net method. Other published papers [13, 16] also discuss the dimension problem. Bases are constructed in [5, 9, 17].

Communicated by: T. Lyche

✉ Jiansong Deng
dengjs@ustc.edu.cn

[1] School of Mathematical Sciences, University of Science and Technology of China, Hefei, China

[2] School of Mathematics, Hefei University of Technology, Hefei, China

Published online: 27 April 2016

For spline spaces with high-order smoothness, the situation becomes more complex. Li et al. discover that the dimensions of spline spaces are dependent on the geometry information of a T-mesh in [18], which is a similar phenomenon as the Morgan-Scott triangulation [7, 21]. Additional examples are given in [1]. The dimensions of spline spaces over some special T-meshes have been discussed in [6, 19, 22, 28, 32].

Previous papers primarily focus on T-meshes whose domains are rectangles without holes. However, we will treat some complex domains that are not rectangles in surface modeling [10, 15, 23] and the finite-element method. We are also confronted with domains with holes [2, 8, 11] in geometry modelling. In isogeometric analysis [14], a central problem is the computation of a reasonable parametric representation for the domain, which is referred to as parameterization; it significantly influences the numerical accuracy and efficiency of the numerical solutions [3]. The traditional computational domain is a rectangle without holes [30]. For the problem of stationary heat conduction in the L-shaped domain shown in Fig. 1 in Section 2 of [31], the authors show that the quality of the parameterization is very low if a single rectangular computational domain is selected. It is because two singular points exist on the boundary when we parameterize the L-shaped domain onto a single rectangular domain. The method in [31] decomposes the L-shaped domain into two subdomains. A non-rectangular (Definition 2.1) computational domain may be another reasonable choice.

The dimensions of spline spaces over T-meshes on arbitrary domains for low-order smoothness have been discussed in [12, 27]. Schumaker et al. discuss spline spaces defined on TR-meshes, which consist of both triangles and rectangles in [26].

In this paper, we discuss the dimensions of spline spaces with high-order smoothness. We present the following results:

1. We provide the dimension formulae of spline spaces over special simply connected T-meshes.
2. We discover a new type of instability of the dimensions.

Fig. 1 L-shaped domain

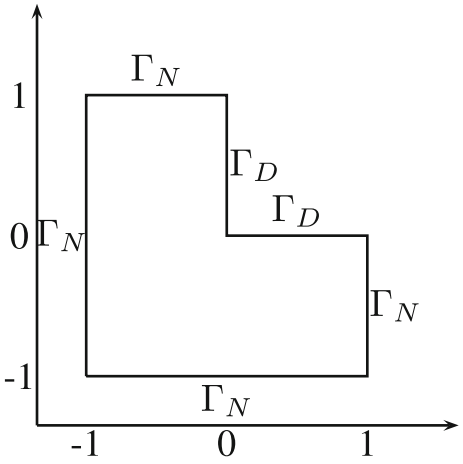

3. We construct a relationship between the spline space over a T-mesh $\mathscr{T}$ with holes and the spline space over a simply connected T-mesh associated with $\mathscr{T}$.

The paper is organized as follows. In Section 2, we define terms that are employed in the following sections. We review the B-net method and the smoothing cofactor method in Section 3. In Section 4, we discuss the dimensions of spline spaces over simply connected T-meshes. In Section 5, the dimensions of spline spaces over T-meshes with holes are discussed. Section 6 provides the conclusions and discusses future studies.

2 Basic definitions

2.1 T-meshes

Definition 2.1 [27] Let $\mathscr{T} := \{C_i\}_{i=1}^{N}$ be a collection of axis-aligned rectangles such that the domain $\Omega(\mathscr{T}) := \bigcup C_i$ is connected. In addition, assume that any pair of distinct rectangles C_i, C_j can only intersect at points on their edges. Then, we call $\mathscr{T}$ a **T-mesh** and C_i a **cell** of $\mathscr{T}$. For a subset I of $\{1, 2, \ldots, N\}$, if $\mathscr{T}' := \{C_i\}_{i\in I}$ is also a T-mesh, we call $\mathscr{T}'$ a **submesh** of $\mathscr{T}$.

If $\Omega(\mathscr{T})$ is a rectangle and simply connected (without holes), we call $\mathscr{T}$ a **rectangular** T-mesh; otherwise, we call it a **non-rectangular** T-mesh.

A vertex of a cell is called a **vertex** of $\mathscr{T}$, and a line segment that connects two adjacent vertices is called an **edge** of $\mathscr{T}$. If a vertex is on the boundary of $\Omega(\mathscr{T})$, it is called a **boundary vertex**; otherwise, it is called an **interior vertex**. Similarly, we have two types of edges: **boundary edges** and **interior edges**. If a cell has a vertex that is a boundary vertex, it is called a **boundary cell**; otherwise, it is called an **interior cell**. T-meshes are allowed to have **T-junctions**, or **T-nodes**, which are the interior vertices of valence three. For two cells C_1, C_2 with a common edge, we say that they are **adjacent**. If a rectangular T-mesh has no T-nodes, it is called a **tensor-product** mesh (TP mesh).

In Fig. 2, $\mathscr{T}_1$ is a rectangular T-mesh, and $\mathscr{T}_2$ and $\mathscr{T}_3$ are non-rectangular T-meshes.

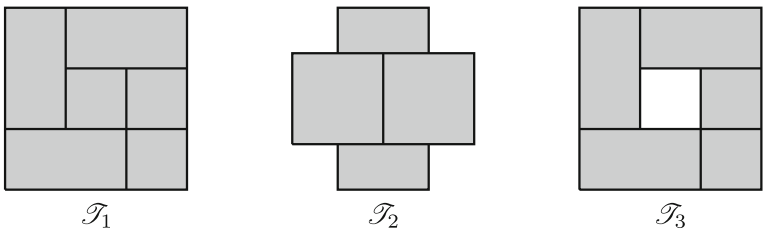

Fig. 2 Three T-meshes

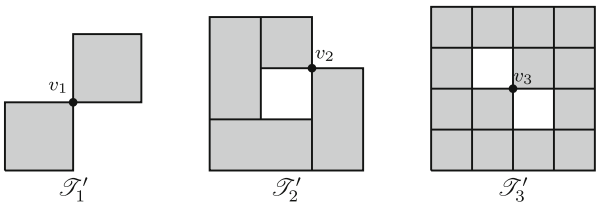

Fig. 3 Three nonregular T-meshes

Definition 2.2 [27] We say that a vertex v is a **regular vertex** provided that the union of all rectangles that contain v has a connected interior. Otherwise, v is a **nonregular vertex**. If a nonregular vertex is on the boundary of a hole, the hole is called a **nonregular hole**.

We say that a T-mesh $\mathscr{T}$ is **regular** provided that every vertex of $\mathscr{T}$ is regular. Otherwise, $\mathscr{T}$ is **nonregular**.

The T-meshes in Fig. 2 are regular. The T-meshes in Fig. 3 are nonregular. The three vertices v_1, v_2 and v_3 in Fig. 3 are nonregular vertices. The three holes in $\mathscr{T}_2'$ and $\mathscr{T}_3'$ are nonregular holes.

Given a T-mesh $\mathscr{T}$, the region $\Omega(\mathscr{T})$ is bounded by the edges of some polygons. We show the regions in Fig. 4 for some T-meshes in Figs. 2 and 3. We see that the region $\Omega(\mathscr{T})$ is bounded by the edges of only simple polygons for a regular T-mesh $\mathscr{T}$, whereas these polygons must include self-intersecting polygons that self-intersect at nonregular vertices for a nonregular T-mesh.

A **large edge** (**L-edge**) is a line segment that consists of several edges (boundary or interior). It is the longest possible line segment, the interior edges of which are connected and the two end points are T-junctions or boundary vertices. If an L-edge only consists of interior edges, it is called an **interior L-edge**; otherwise, it is called a **boundary L-edge**. A **composite edge** (**c-edge**) is a line segment that consists of several *interior* edges. It is the longest possible line segment, the interior edges of which are connected and the two end points are T-junctions or boundary vertices. Three types of c-edges exist. If both end points of a c-edge are T-junctions, the c-edge is called a **T c-edge**. If both end points of a c-edge are boundary vertices, the c-edge is called a **cross-cut**. If one end point is a boundary vertex and the other end point is a T-junction, the c-edge is called a **ray**.

We classify boundary vertices and c-edges more specifically for a simply connected regular T-mesh $\mathscr{T}$. The region $\Omega(\mathscr{T})$ is a polygon whose interior angles

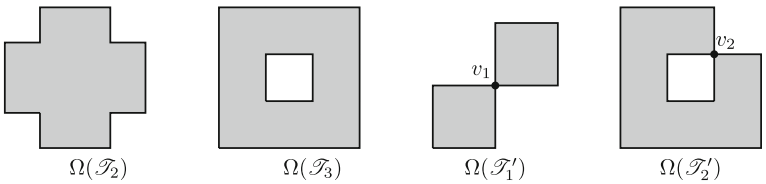

Fig. 4 The regions occupied by the T-meshes

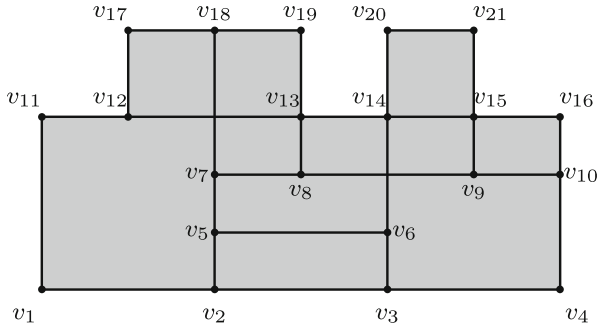

Fig. 5 A simply connected regular T-mesh $\mathscr{T}$

are 90° or 270°. We call the boundary vertices corresponding to 90° interior angles and 270° interior angles **convex vertices** and **concave vertices**, respectively. The remaining boundary vertices are called **flat vertices**. For the T-mesh in Fig. 5, $v_1, v_4, v_{16}, v_{21}, v_{20}, v_{19}, v_{17}, v_{11}$ are convex vertices, $v_{15}, v_{14}, v_{13}, v_{12}$ are concave vertices, and v_2, v_3, v_{10}, v_{18} are flat vertices. Assume l is a cross-cut. The end points of l may be flat vertices or concave vertices. If both end points of l are flat vertices, we call l a **flat cross-cut**; if both end points of l are concave vertices, we call l a **concave cross-cut**; if one end point of l is a concave vertex and the other end point is a flat vertex, we call l a **concave-flat cross-cut**. For the T-mesh in Fig. 5, the cross-cut between v_2 and v_{18} is the only flat cross-cut, the cross-cut between v_3 and v_{14} is the only concave-flat cross-cut, and the cross-cut between v_{14} and v_{15} and the cross-cut between v_{12} and v_{13} are concave cross-cuts. Assume l' is a ray. One end point of l' is a T-junction and the other end point can be a flat vertex or a concave vertex. If one end point of l' is a flat vertex, l' is called a **flat ray**; if one end point of l' is a concave vertex, l' is called a **concave ray**. For the T-mesh in Fig. 5, the ray between v_8 and v_{13} and the ray between v_9 and v_{15} are concave rays, and the ray between v_7 and v_{10} is the only flat ray.

Definition 2.3 If a simply connected regular T-mesh $\mathscr{T}$ has no T c-edges in $\mathscr{T}$, we call $\mathscr{T}$ a **quasi-cross-cut** T-mesh.

Now, we introduce some notations for a T-mesh in Table 1.

Lemma 2.4 *Given a simply connected regular T-mesh $\mathscr{T}$ with the notations in* Table 1*, it follows that*

1. $E^i = G_f + R_f + T$;
2. $V_f^b = 2G_f + G_{af} + R_f$;
3. $V_e^b + V_a^b = E^b + G_a$;
4. *if $\mathscr{T}$ is a quasi-cross-cut T-mesh, then $V^b = E + G$.*

Table 1 Notations for a T-mesh

V	number of vertices
V^b	number of boundary vertices
V^i	number of interior vertices
V_e^b	number of convex vertices
V_a^b	number of concave vertices
V_f^b	number of flat vertices
E	number of L-edges
E^b	number of boundary L-edges
E^i	number of interior L-edges
G	number of cross-cuts
G_f	number of flat cross-cuts
G_a	number of concave cross-cuts
G_{af}	number of concave-flat cross-cuts
R	number of rays
R_f	number of flat rays
R_a	number of concave rays
T	number of T c-edges

Proof

1. An interior L-edge can be a flat cross-cut, a flat ray, or a T c-edge. Therefore, this conclusion is correct.
2. Every flat vertex is an end point of a ray or a cross-cut. By the definitions of these c-edges, the conclusion can be easily obtained.
3. After deleting all flat cross-cuts, concave-flat cross-cuts, rays and T c-edges, we obtain the submesh $\mathscr{T}'$ of $\mathscr{T}$. For the T-mesh $\mathscr{T}$ in Fig. 5, the mesh $\mathscr{T}'$ in Fig. 6 is the obtained submesh. After deleting all concave cross-cuts of $\mathscr{T}'$, we obtain the submesh $\mathscr{T}''$ which only has one cell. The mesh $\mathscr{T}''$ in Fig. 6 is the obtained submesh. To express the distinction, we employ $V^b(\mathscr{T}')$, $V^b(\mathscr{T}'')$, etc to denote the number of boundary vertices of $\mathscr{T}'$, the number of boundary vertices of $\mathscr{T}''$, etc. We have

$$V_e^b + V_a^b = V^b(\mathscr{T}') = V^b(\mathscr{T}''),\ E^b = E^b(\mathscr{T}'),\ G_a = G_a(\mathscr{T}').$$

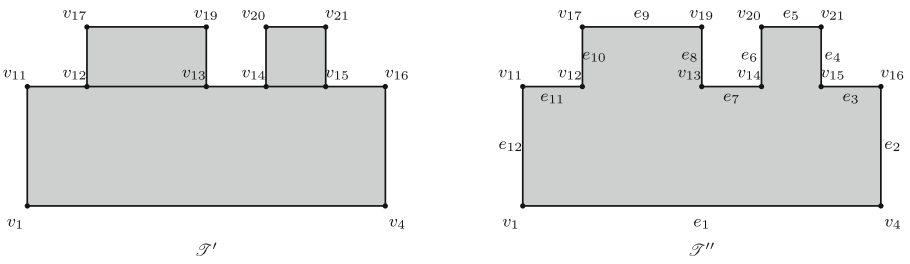

Fig. 6 Two submeshes of $\mathscr{T}$ in Fig. 5

Because $\mathscr{T}$ is regular, the boundary edges of $\Omega(\mathscr{T}'')$ are not self-intersecting. Therefore, we obtain $E^b(\mathscr{T}'') = V^b(\mathscr{T}'')$.

We claim that $E^b(\mathscr{T}') + G_a(\mathscr{T}') = E^b(\mathscr{T}'')$. Two situations exist in what the boundary L-edges of $\mathscr{T}'$ may become in $\mathscr{T}''$. The first situation is that a boundary L-edge of $\mathscr{T}'$ remains a boundary L-edge in $\mathscr{T}''$. For the mesh $\mathscr{T}'$ in Fig. 6, the boundary L-edge between v_1 and v_4, the boundary L-edge between v_4 and v_{16}, the boundary L-edge between v_{20} and v_{21}, etc become e_1, e_2, e_5, etc in $\mathscr{T}''$. In the second situation, if k concave cross-cuts exist on a boundary L-edge of $\mathscr{T}'$, this boundary L-edge will become $k+1$ boundary L-edges in $\mathscr{T}''$. For example, the boundary L-edge between v_{11} and v_{16} becomes e_{11}, e_7, e_3 in $\mathscr{T}''$. Therefore, this claim is correct.

Combining these relationships, we complete the proof.

4. If $\mathscr{T}$ is a quasi-cross-cut T-mesh, then $T = 0$. By the last three relationships, it follows that

$$\begin{aligned} V^b &= V_f^b + V_e^b + V_a^b \\ &= 2G_f + G_{af} + R_f + E^b + G_a \\ &= (G_f + R_f) + E^b + (G_f + G_{af} + G_a) \\ &= E^i + E^b + G \\ &= E + G. \end{aligned}$$

□

Definition 2.5 Suppose $\mathscr{T}$ is a TP mesh. After deleting some cells of $\mathscr{T}$, we obtain a submesh of $\mathscr{T}$. We call this mesh a **quasi-TP mesh**.

Figure 7 shows two examples of quasi-TP meshes.

2.2 Spline spaces over T-meshes

Given a T-mesh $\mathscr{T} = \{C_i\}_{i=1}^N$, in [6], the following two spline spaces are defined as:

$$\mathbf{S}(m,n,\alpha,\beta,\mathscr{T}) := \{f(x,y) \in C^{\alpha,\beta}(\Omega(\mathscr{T})) : f(x,y)|_{C_i} \in \mathbb{P}_{mn} \text{ for any } C_i \in \mathscr{T}\},$$

$$\overline{\mathbf{S}}(m,n,\alpha,\beta,\mathscr{T}) := \{f(x,y) \in C^{\alpha,\beta}(\mathbb{R}^2) : f(x,y)|_{C_i} \in \mathbb{P}_{mn} \text{ for any } C_i \in \mathscr{T} \text{ and } f|_{\mathbb{R}^2 \setminus \Omega(\mathscr{T})} \equiv 0\},$$

Fig. 7 Two quasi-TP meshes

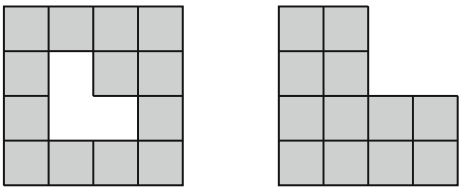

where $\mathbb{P}_{mn} = \{p(x, y) : p(x, y) = \sum_{i=0}^{m} \sum_{j=0}^{n} c_{ij} x^i y^j, c_{ij} \in \mathbb{R}\}$ and $C^{\alpha,\beta}$ is the space consisting of all bivariate functions continuous with order α along x-direction and with order β along y-direction. The space $\mathbf{S}(m, n, \alpha, \beta, \mathscr{T})$ is called a spline space over $\mathscr{T}$, while $\overline{\mathbf{S}}(m, n, \alpha, \beta, \mathscr{T})$ is called a spline space over $\mathscr{T}$ with homogeneous boundary conditions.

Both $\mathbf{S}(m, n, \alpha, \beta, \mathscr{T})$ and $\overline{\mathbf{S}}(m, n, \alpha, \beta, \mathscr{T})$ are linear spaces. In this paper, we only discuss $\mathbf{S}(d, d, d-1, d-1, \mathscr{T})$ and $\overline{\mathbf{S}}(d, d, d-1, d-1, \mathscr{T})$, which are denoted as $\mathbf{S}_d(\mathscr{T})$ and $\overline{\mathbf{S}}_d(\mathscr{T})$ for convenience.

Remark 2.6 The definition of spline spaces over T-meshes in [27] is a little different, where that $f \in C^{\alpha,\beta}(\Omega(\mathscr{T}))$ means the mixed derivatives $\frac{\partial^{i+j} f}{\partial x^i \partial y^j}$ are continuous for all $0 \leqslant i \leqslant \alpha$ and $0 \leqslant j \leqslant \beta$. The definition that we adopt in this paper is more popular in the literature.

3 The B-net method and the smoothing cofactor method

In this section, we review the B-net method and the smoothing cofactor method for computing the dimensions of spline spaces.

3.1 The B-net method

The B-net method is based on the Bernstein-Bézier representation of polynomials. Refer to [4, 27] for details.

For two adjacent cells $C_1 : [x_0, x_1] \times [y_0, y_1]$ and $C_2 : [x_1, x_2] \times [y_2, y_3]$ (refer to Fig. 8, the left cell is C_1), f_1, f_2, respectively, are two polynomials defined on the two cells. The Bernstein-Bézier forms of the two polynomials are:

$$f_1 = \sum_{i,j=0}^{d} c_{i,j} \mathbf{B}_i^d\left(\frac{x - x_0}{x_1 - x_0}\right) \mathbf{B}_j^d\left(\frac{y - y_0}{y_1 - y_0}\right),$$

$$f_2 = \sum_{i,j=0}^{d} c'_{i,j} \mathbf{B}_i^d\left(\frac{x - x_1}{x_2 - x_1}\right) \mathbf{B}_j^d\left(\frac{y - y_1}{y_2 - y_1}\right),$$

where $\mathbf{B}_i^d(t)$ and $\mathbf{B}_j^d(t)$ are the Bernstein polynomials, and $c_{i,j}$ and $c'_{i,j}$ are the **B-coefficients** of the two polynomials.

The B-coefficient $c_{i,j}$ corresponds to the point $(\frac{(d-i)x_0 + ix_1}{d}, \frac{(d-j)y_0 + jy_1}{d})$, which is called a **domain point** associated with C_1. The domain points of C_1 and C_2 are denoted by "$\bullet$" and "$\circ$", respectively, for the case $d = 3$ in Fig. 8.

When $c_{i,j}, 1 \leqslant i \leqslant d, 0 \leqslant j \leqslant d$ are given, the smoothness conditions indicate that $c'_{i,j}, 0 \leqslant i \leqslant d-1, 0 \leqslant j \leqslant d$ are determined. As shown in Fig. 8, when the B-coefficients corresponding to the domain points in the last three columns of C_1 are given, the B-coefficients corresponding to the domain points in the first three columns of C_2 are determined.

Fig. 8 The B-net method

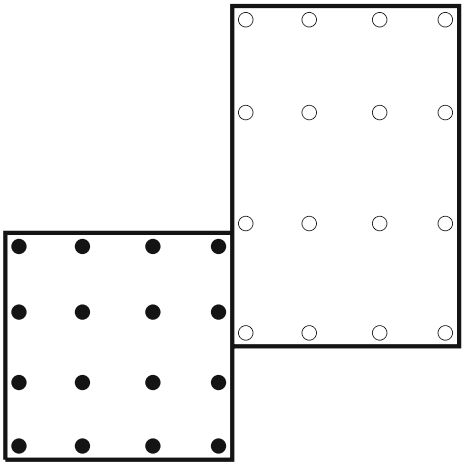

If the common edge that belongs to the two adjacent cells is a horizontal edge, the conclusions are similar. For a spline space $\mathbf{S}_d(\mathscr{T})$, $\mathscr{D}$ is the set of all domain points of $\mathscr{T}$. For a subset $\mathscr{P} \subseteq \mathscr{D}$ and a function $f \in \mathbf{S}_d(\mathscr{T})$, suppose $C(\mathscr{P}, f)$ is the set of the B-coefficients of f, which corresponds to all elements of $\mathscr{P}$. The set $\mathscr{P}$ is called a **determining set** of $\mathbf{S}_d(\mathscr{T})$ if for any function $f \in \mathbf{S}_d(\mathscr{T})$,

$$c = 0, \quad \forall c \in C(\mathscr{P}, f) \Rightarrow f = 0.$$

If any nontrivial subset of $\mathscr{P}$ is not a determining set, we call $\mathscr{P}$ a **minimal determining set** of $\mathbf{S}_d(\mathscr{T})$. We have

$$\dim \mathbf{S}_d(\mathscr{T}) = \#\mathscr{P},$$

where $\#\mathscr{P}$ is the number of elements of $\mathscr{P}$.

3.2 The smoothing cofactor method

The smoothing cofactor method was first introduced in [24] and [29]. This method has been discussed in more detail in [16, 19, 28].

Suppose $\mathbf{S}_d(\mathscr{T})$ is a spline space defined on $\mathscr{T}$ and $f \in \mathbf{S}_d(\mathscr{T})$. For two adjacent cells C_1 and C_2, assume that $f|_{C_1} = f_1$, $f|_{C_2} = f_2$ and the common edge of C_1 and C_2 is on the line $x = x_0$. There exists a polynomial $a(y) \in \mathbb{P}_d[y]$, such that

$$f_1 - f_2 = a(y)(x - x_0)^d.$$

Similarly, if the common edge of C_1 and C_2 is on the line $y = y_0$. There exists a polynomial $b(x) \in \mathbb{P}_d[x]$, such that

$$f_1 - f_2 = b(x)(y - y_0)^d.$$

The polynomial $a(y)$ or $b(x)$ is called the **edge cofactor** of the common edge.

Suppose $\mathscr{E}$ is the set of all interior edges of $\mathscr{T}$. For an interior edge e, we use $c(e)$ to denote the edge cofactor of e. Then we obtain a linear space

$$C(\mathscr{E}) := \{(c(e_1), c(e_2), \ldots, c(e_N)) : e_i \in \mathscr{E}\},$$

where N is the number of elements in $\mathscr{E}$. If $\mathscr{T}$ is a regular T-mesh, then

$$\dim \mathbf{S}_d(\mathscr{T}) = (d+1)^2 + \dim C(\mathscr{E}). \tag{1}$$

3.2.1 Local conformality condition of edge cofactors

For an interior vertex, we have the following conformality condition.

Referring to Fig. 9, let $f_j(x, y)$, $j = 1, 2, 3, 4$ be the bivariate polynomials surrounding the interior vertex $v_i(x_i, y_i)$ (if the vertex v_i is a T-junction, some of the polynomials are identical). Then there exist four polynomials $a_1(y), a_2(y) \in \mathbb{P}_d[y]$, $b_1(x), b_2(x) \in \mathbb{P}_d[x]$, such that

$$\begin{aligned} f_1(x, y) - f_2(x, y) &= b_1(x)(y - y_i)^d, \\ f_2(x, y) - f_3(x, y) &= a_1(y)(x - x_i)^d, \\ f_3(x, y) - f_4(x, y) &= b_2(x)(y - y_i)^d, \\ f_4(x, y) - f_1(x, y) &= a_2(y)(x - x_i)^d, \end{aligned}$$

where $a_1(y), a_2(y), b_1(x), b_2(x)$ are the edge cofactors associated with the corresponding edges. Adding these four equations, we obtain

$$(b_1(x) + b_2(x))(y - y_i)^d + (a_1(y) + a_2(y))(x - x_i)^d = 0.$$

Because $a_1(y), a_2(y) \in \mathbb{P}_d[y]$, $b_1(x), b_2(x) \in \mathbb{P}_d[x]$, there exist a constant $\gamma_i \in \mathbb{R}$, such that

$$(b_1(x) + b_2(x)) = \gamma_i (x - x_i)^d, \quad (a_1(y) + a_2(y)) = -\gamma_i (y - y_i)^d,$$

and γ_i is the **vertex cofactor** associated with the vertex v_i.

For a regular hole in a T-mesh, we have another conformality condition. Refer to Fig. 10 for a simple example.

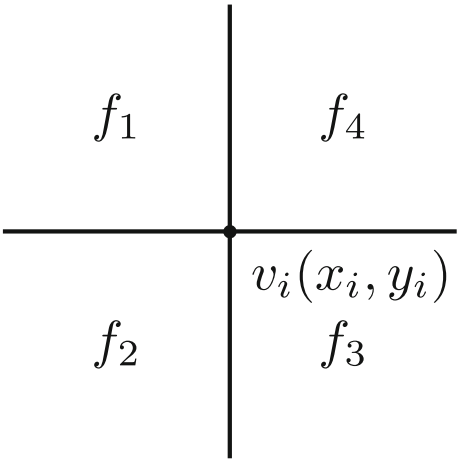

Fig. 9 Smoothing conditions around an interior vertex

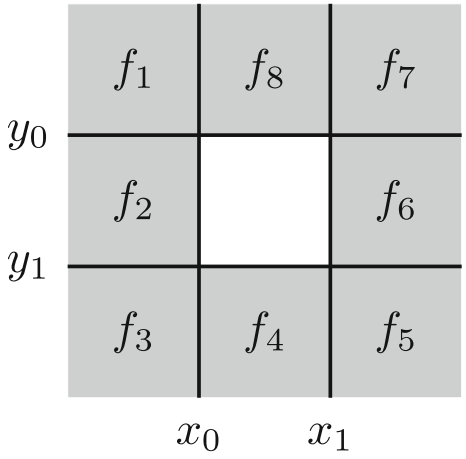

Fig. 10 Smoothing conditions around a regular hole

Suppose the two horizontal lines are $y = y_0$ and $y = y_1$, and the two vertical lines are $x = x_0$ and $x = x_1$. We have

$$\begin{aligned} f_1 - f_2 &= h_1(x)(y - y_0)^d, \\ f_2 - f_3 &= h_2(x)(y - y_1)^d, \\ &\vdots \\ f_8 - f_1 &= v_4(y)(x - x_0)^d, \end{aligned}$$

where $h_1(x), \ldots, h_4(x)$ are the edge cofactors corresponding to the four horizontal edges in counter-clockwise direction, and $v_1(x), \ldots, v_4(x)$ are the edge cofactors corresponding to the four vertical edges in counter-clockwise direction. Adding these equations, we obtain

$$\begin{aligned} &(h_1(x) + h_4(x))(y - y_0)^d + (h_2(x) + h_3(x))(y - y_1)^d + \\ &(v_1(y) + v_4(y))(x - x_0)^d + (v_2(y) + v_3(y))(x - x_1)^d = 0. \end{aligned} \tag{2}$$

This condition is similar to the condition in Theorem 9.3 of [25]. However, the four lines do not insect at a vertex. Therefore, the conclusion in [25] does not apply here. Analyzing Equation (2) is not a trivial task. We seek alternate methods to analyze the dimension when $\mathscr{T}$ has holes.

3.3 Regular T-meshes and nonregular T-meshes

Lemma 3.1 *Given a regular T-mesh $\mathscr{T}$, it follows that*

$$\mathbf{S}_d(\mathscr{T}) \subseteq C^{d-1}(\Omega(\mathscr{T}))$$

Proof We prove this lemma for $\mathbf{S}_3(\mathscr{T})$; other situations can be proved similarly.

We only need to prove that, for any vertex v, if v belongs to more than one cell, any function $f \in \mathbf{S}_3(\mathscr{T})$ is C^2 continuous at v. Because $\mathscr{T}$ is regular, v must belong to two adjacent cells C_1, C_2. Without losing generality, we assume that the common

edge of C_1, C_2 is on the line $x = 0$ and the coordinate of v is $(0, y_0)$. To prove that f is C^2 continuous at v, we should prove that $\frac{\partial^2 f}{\partial x^2}, \frac{\partial^2 f}{\partial y^2}, \frac{\partial^2 f}{\partial x \partial y}$ are continuous at v. Because $f \in C^{2,2}(\Omega(\mathscr{T}))$, $\frac{\partial^2 f}{\partial x^2}, \frac{\partial^2 f}{\partial y^2}$ are both continuous. Now, we prove that $\frac{\partial^2 f}{\partial x \partial y}$ is also continuous.

Suppose $f_1 = f|_{C_1}$, $f_2 = f|_{C_2}$. We need to prove that $\frac{\partial^2 f_1}{\partial x \partial y}(0, y_0) = \frac{\partial^2 f_2}{\partial x \partial y}(0, y_0)$. We have

$$\frac{\partial^2 f_1}{\partial x \partial y}(0, y_0) = \lim_{h \to 0} \frac{\frac{\partial f_1}{\partial x}(0, y_0 + h) - \frac{\partial f_1}{\partial x}(0, y_0)}{h}, \quad \frac{\partial^2 f_2}{\partial x \partial y}(0, y_0) = \lim_{h \to 0} \frac{\frac{\partial f_2}{\partial x}(0, y_0 + h) - \frac{\partial f_2}{\partial x}(0, y_0)}{h}.$$

Because $f \in C^{2,2}(\Omega(\mathscr{T}))$, $\frac{\partial f_1}{\partial x}(0, y_0 + h) = \frac{\partial f_2}{\partial x}(0, y_0 + h)$ and $\frac{\partial f_1}{\partial x}(0, y_0) = \frac{\partial f_2}{\partial x}(0, y_0)$. Therefore, $\frac{\partial^2 f_1}{\partial x \partial y}(0, y_0) = \frac{\partial^2 f_2}{\partial x \partial y}(0, y_0)$, which proves this lemma. □

If $\mathscr{T}$ is nonregular, the continuity of $\frac{\partial^2 f}{\partial x \partial y}$ can not be guaranteed for nonregular vertices, which indicates that $\mathbf{S}_3(\mathscr{T}) \nsubseteq C^2(\Omega(\mathscr{T}))$. To explain the difference, we construct another spline space:

$$\mathbb{S}_d(\mathscr{T}) := \{f(x, y) \in C^{d-1}(\Omega(\mathscr{T})) : f(x, y)|_{C_i} \in \mathbb{P}_{dd} \text{ for all } i = 1, 2, \ldots, N\},$$

where $C_1, C_2, \ldots, C_N$ are all cells of $\mathscr{T}$.

Restricted to $d = 3$, for the T-mesh $\mathscr{T}_1'$ in Fig. 3, we can easily obtain the minimal determining set of $\mathbf{S}_3(\mathscr{T}_1')$, which is shown in Fig. 11. For $\mathbb{S}_3(\mathscr{T}_1')$, $\frac{\partial^2 f}{\partial x \partial y}$ should be continuous at v_1. By Lemma 3.3 of [27], the number of elements of the minimal determining set of $\mathbb{S}_3(\mathscr{T}_1')$ is one less than that of $\mathbf{S}_3(\mathscr{T}_1')$, which is shown in Fig. 11. We obtain $\dim \mathbf{S}_3(\mathscr{T}_1') = 27$ and $\dim \mathbb{S}_3(\mathscr{T}_1') = 26$.

4 Simply connected regular T-meshes

4.1 Conformality vector space

For each interior edge in a simply connected mesh $\mathscr{T}$, at least one end point is an interior vertex. Suppose $\mathscr{V}$ is the set of all interior vertices of $\mathscr{T}$. For an interior vertex v, we use $c(v)$ to denote the vertex cofactor of v. Then, we obtain a linear space

$$C(\mathscr{V}) := \{(c(v_1), c(v_2), \ldots, c(v_M)) : v_i \in \mathscr{V}\},$$

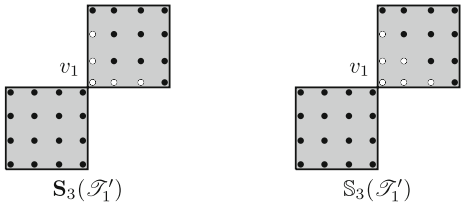

Fig. 11 Minimal determining sets (labelled by "•") of the two spline spaces

where M is the number of elements in $\mathscr{V}$. We know that

$$\dim C(\mathscr{E}) = (d+1)G + \dim C(\mathscr{V}), \tag{3}$$

where G is the number of cross-cuts of $\mathscr{T}$.

The conformality condition of vertex cofactors is based on T c-edges. The detailed derivation is provided in [16, 19, 28]. Here we only list the conclusions.

Given a horizontal T c-edge l_j with r vertices $v_{j_1}, v_{j_2}, \ldots, v_{j_r}$, let the x-coordinate of v_{j_i} be x_{j_i}, and the vertex cofactor of v_{j_i} be γ_{j_i}. Then

$$\sum_{i=1}^{r} \gamma_{j_i} (x - x_{j_i})^d = 0.$$

This equation is equivalent to the linear system denoted by $\mathscr{S}_{l_j} = 0$:

$$\begin{cases} \sum_{i=1}^{r} \gamma_{j_i} = 0, \\ \sum_{i=1}^{r} \gamma_{j_i} x_{j_i} = 0, \\ \cdots, \\ \sum_{i=1}^{r} \gamma_{j_i} x_{j_i}^d = 0. \end{cases} \tag{4}$$

Similarly, we can derive a linear system for a vertical T c-edge.

As shown in [28], we can define the conformality vector space for a set of T c-edges as follows.

Definition 4.1 Suppose L is a set of T c-edges: $L = \{l_1, l_2, \ldots, l_n : l_i \text{ is a T c-edge}, 1 \leqslant i \leqslant n\}$, $v_1, v_2, \ldots, v_m$ are all vertices on $l_1, l_2, \ldots, l_n$, and γ_j is the vertex cofactor of v_j. Then the **conformality vector space** $W[L]$ of L is defined by

$$W[L] := \{\gamma = (\gamma_1, \gamma_2, \ldots, \gamma_m)^T : \mathscr{S}_{l_i} = 0,\ 0 \leqslant i \leqslant n\},$$

where $\mathscr{S}_{l_i} = 0$ is the linear system as Eq. (4) associated with the T c-edge l_i. For some predefined ordering of the vertex cofactors and the T c-edges, the coefficient matrix for the homogeneous system of $W[L]$ is called the **conformality matrix** of L.

Combining Equation (1) and Equation (3), we obtain the following lemma, which is also elaborated in [16].

Lemma 4.2 *Given a simply connected T-mesh $\mathscr{T}$ with G cross-cuts and V^i interior vertices, let M be the conformality matrix of all of the T c-edges. Then,*

$$\dim \mathbf{S}_d(\mathscr{T}) = (d+1)^2 + (d+1)G + V^i - \operatorname{rank} M.$$

Remark 4.3 For a given T-mesh $\mathscr{T}$, we use $\mathscr{C}(\mathscr{T})$ to denote the set of all T c-edges in $\mathscr{T}$. Then, Lemma 4.2 states that

$$\dim \mathbf{S}_d(\mathscr{T}) = \dim W[\mathscr{C}(\mathscr{T})] + \dim \mathbf{S}_d(\mathscr{T} \backslash \mathscr{C}(\mathscr{T})). \tag{5}$$

Here, $\mathscr{T} \backslash \mathscr{C}(\mathscr{T})$ is the mesh obtained by deleting $\mathscr{C}(\mathscr{T})$ from $\mathscr{T}$.

If the spline space is $\overline{\mathbf{S}}_d(\mathscr{T})$, then for any *L-edge* l of $\mathscr{T}$, the vertex cofactors of all vertices on l satisfy the linear system $\mathscr{S}_l = 0$ as Equation (4). Therefore, we can

define the conformality vector space $W[\mathscr{L}(\mathscr{T})]$, which is similar to Definition 4.1, where $\mathscr{L}(\mathscr{T})$ denotes the set of all L-edges of $\mathscr{T}$. We have the following lemma:

Lemma 4.4 ([28])

$$\overline{\mathbf{S}}_d(\mathscr{T}) \cong W[\mathscr{L}(\mathscr{T})].$$

4.2 Dimensions of spline spaces over simply connected T-meshes

Lemma 4.5 *Given a quasi-cross-cut T-mesh $\mathscr{T}$, it follows that*

$$\dim \mathbf{S}_d(\mathscr{T}) = V + dV^b - (d+1)E + (d+1)^2,$$

where V, V^b, E are defined in Table 1.

Proof By Lemma 4.2 and Lemma 2.4, we have

$$\begin{aligned}\dim \mathbf{S}_d(\mathscr{T}) &= (d+1)^2 + (d+1)G + V^i \\ &= (d+1)^2 + (d+1)(V^b - E) + V - V^b \\ &= V + dV^b - (d+1)E + (d+1)^2.\end{aligned}$$

□

If $\mathscr{T}$ contains T c-edges, the dimension problem becomes very difficult. Some discussions are provided in [19, 22, 32]. We list the following definition and lemma which will be presented in the following sections.

Definition 4.6 Given a T-mesh $\mathscr{T}$, let $L = \{l_1, l_2, \ldots, l_n\}$ be a set of T c-edges. If there is an ordering of all T c-edges of L, such as $l_1, l_2, \ldots, l_n$, such that $n_{l_i} \geqslant d+1$, where n_{l_i} is the number of vertices on l_i but not on l_j, $j = 1, 2, \ldots, i-1$, then we say L has a **reasonable ordering**.

Lemma 4.7 ([32]) *Suppose $L = \{l_1, l_2, \ldots, l_n\}$ is a set of T c-edges which has a reasonable ordering. Then*

$$\dim W[L] = V_L - (d+1)n,$$

where V_L is the number of vertices on all T c-edges of L.

If the spline space is $\overline{\mathbf{S}}_d(\mathscr{T})$, Definition 4.6 and Lemma 4.7 should be revised for L-edges instead of T c-edges, as discussed in Section 4.1.

Combining Equation (5), Lemma 4.5 and Lemma 4.7, we obtain the following theorem.

Theorem 4.8 *Given a simply connected T-mesh $\mathscr{T}$, if $\mathscr{C}(\mathscr{T})$ has a reasonable ordering, then*

$$\dim \mathbf{S}_d(\mathscr{T}) = V + dV^b - (d+1)E + (d+1)^2,$$

where V, V^b, E are defined in Table 1.

If the set $\mathscr{C}(\mathscr{T})$ does not have a reasonable ordering, the dimension may be unstable. In Fig. 12, we can check that $\dim \mathbf{S}_3(\mathscr{T}) = 48$ or 49 for the same conditions for the four T c-edges in [18].

5 T-meshes with holes

First, we give a T-mesh with a hole, over which the dimension of the spline space is unstable.

See the non-rectangular T-mesh $\mathscr{T}$ in Fig. 13, where x_1 and x_2 are the x-coordinates of the two vertical edges. In Section 3.2.1, we have discussed the local conformality condition of the edge cofactors around the holes. We can express the conformality equations as Equation (2) for the two situations in which $x_1 = x_2$ and $x_1 \neq x_2$. We do not list the equations to save space. With the help of Maple, we determine that if $x_1 = x_2$, $\dim \mathbf{S}_3(\mathscr{T}) = 42$; otherwise, $\dim \mathbf{S}_3(\mathscr{T}) = 40$.

We have mentioned that the analysis of the conformality equation expressed as Equation (2) is not a trivial task. Therefore, directly computing the dimension by the smoothing cofactor method is not a wise choice. A more reasonable idea is to construct the relationship between a T-mesh with holes and a T-mesh without holes.

Suppose there are H holes in $\mathscr{T}$. We use $\Omega_1, \Omega_2, \ldots, \Omega_H$ and $C_1^0, C_2^0, \ldots, C_H^0$ to denote the regions occupied by these holes and the polygons bounded by the boundaries of $\Omega_1, \Omega_2, \ldots, \Omega_H$. The edges of C_i^0 are axis-aligned lines and C_i^0 may be not a rectangle. We use Ω^0 and $\mathscr{T}^s$ to denote $\bigcup_{i=1}^H \Omega_i$ and the mesh $\mathscr{T} \cup \{C_i^0\}_{i=1}^H$, respectively. The mesh $\mathscr{T}^s$ is called the **simply connected mesh corresponding to** $\mathscr{T}$. See Fig. 14 for an example. If $C_1^0, C_2^0, \ldots, C_H^0$ are all rectangles, $\mathscr{T}^s$ is also a T-mesh. Similarly, we can define $\mathbf{S}_d(\mathscr{T}^s)$ and $\overline{\mathbf{S}}_d(\mathscr{T}^s)$.

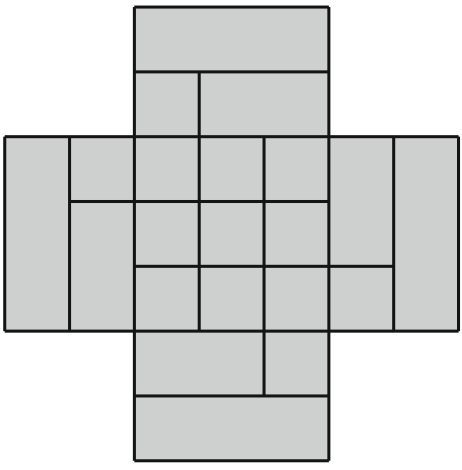

Fig. 12 Simply connected nonrectangle T-mesh $\mathscr{T}$

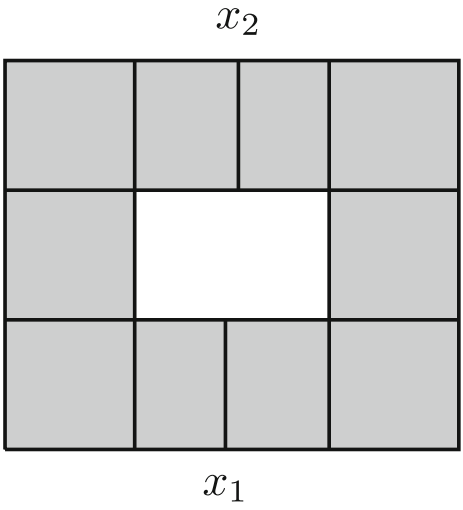

Fig. 13 A T-mesh $\mathscr{T}$ with a hole

Lemma 5.1 *Suppose C is a simple polygon whose edges are axis-aligned lines and $\mathscr{C} = \{C\}$ is a mesh that only has one cell C. Then*

$$\dim \overline{\mathbf{S}}_d(\mathscr{C}) = 0.$$

Proof The cell C has at least two horizontal edges which are located on the lines $y = y_1, y = y_2$ $(y_1 \neq y_2)$ and two vertical edges which are located on the lines $x = x_1, x = x_2$ $(x_1 \neq x_2)$. By the discussion in Section 3.2.1, for any $f(x, y) \in \overline{\mathbf{S}}_d(\mathscr{C})$, there exist $a_1(y), a_2(y) \in \mathbb{P}_d[y], b_1(x) \in \mathbb{P}_d[x]$, such that

$$f(x, y) = a_1(y)(x-x_1)^d, \qquad f(x, y) = a_2(y)(x-x_2)^d, \qquad f(x, y) = b_2(x)(y-y_1)^d.$$

Therefore, $b_2(x)(y - y_1)^d = a_1(y)(x - x_1)^d$, $b_2(x)(y - y_1)^d = a_2(y)(x - x_2)^d$. There exist $k_1, k_2 \in \mathbb{R}$, such that $b_2(x) = k_1(x-x_1)^d = k_2(x-x_2)^d$. Since $(x-x_1)^d$ and $(x - x_2)^d$ are prime to each other, we obtain $k_1 = k_2 = 0$, which indicates that $f(x, y) = 0$. □

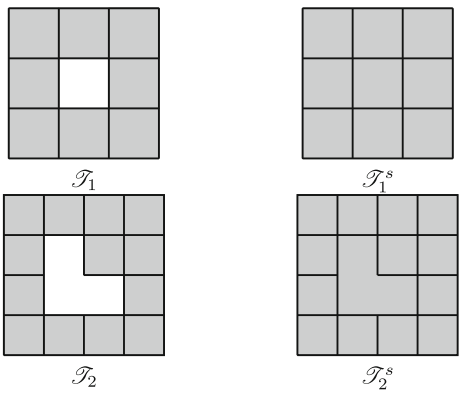

Fig. 14 T-meshes with holes

Lemma 5.2

$$\dim \mathbf{S}_d(\mathscr{T}) \geqslant \dim \mathbf{S}_d(\mathscr{T}^s).$$

Proof We construct the mapping

$$\begin{aligned} \pi: \quad \mathbf{S}_d(\mathscr{T}^s) &\longrightarrow \mathbf{S}_d(\mathscr{T}) \\ f &\longmapsto f|_{\Omega(\mathscr{T})}. \end{aligned}$$

For any $f \in \operatorname{Ker}\pi$, $f|_{\Omega(\mathscr{T})} = 0$. By Lemma 5.1, $f|_{\Omega_i} = 0$. Therefore, $f|_{\Omega(\mathscr{T}^s)} = 0$, that is, $\operatorname{Ker}\pi = 0$ and π is injective. Therefore, $\dim \mathbf{S}_d(\mathscr{T}^s) \leqslant \dim \mathbf{S}_d(\mathscr{T})$. □

From Lemma 5.2, we know that the dimension problem is solved if the mapping π is surjective. If the mapping π is surjective, for any function $f \in \mathbf{S}_d(\mathscr{T})$, we can find a function $f' \in \mathbf{S}_d(\mathscr{T}^s)$, such that $f'|_{\Omega(\mathscr{T})} = f$, that is, f can be **extended** to Ω^0. We call f' the **extension** of f on $\Omega(\mathscr{T}^s)$. If π is surjective, $\mathbf{S}_d(\mathscr{T}^s)$ is called the **extension space** of $\mathbf{S}_d(\mathscr{T})$. Therefore, the dimension problem becomes an extension problem.

Lemma 5.3 *For the T-meshes $\mathscr{T}$ and $\mathscr{T}^0$ in Fig. 15, any function $f \in \mathbf{S}_d(\mathscr{T})$ can be extended to $\Omega(\mathscr{T}^0)$.*

Proof For the mapping

$$\begin{aligned} \pi: \quad \mathbf{S}_d(\mathscr{T}^0) &\longrightarrow \mathbf{S}_d(\mathscr{T}) \\ f &\longmapsto f|_{\Omega(\mathscr{T})}, \end{aligned}$$

we prove that π is surjective.

By Lemma 4.5, we obtain that $\dim \mathbf{S}_d(\mathscr{T}) = d^2 + 4d + 3$, $\dim \mathbf{S}_d(\mathscr{T}^0) = d^2 + 4d + 4$. For any function $f \in \operatorname{Ker}\pi$, by the B-net method, f has only one B-coefficient (corresponding to the top-right domain point of the top-right cell of $\mathscr{T}^0$) that is nonzero. Therefore, $\dim \operatorname{Ker}\pi = 1$.

We obtain $\dim \mathbf{S}_d(\mathscr{T}^0) = \dim \operatorname{Ker}\pi + \dim \mathbf{S}_d(\mathscr{T})$, which indicates that π is surjective. □

For the nonregular T-mesh $\mathscr{T}_1$ in Fig. 16, the extension of all functions in $\mathbf{S}_3(\mathscr{T}_1)$ to $\Omega(\mathscr{T}_1^0)$ is impossible. From the previous discussion, we know that $\dim \mathbf{S}_3(\mathscr{T}_1) = 27$ and $\dim \mathbf{S}_3(\mathscr{T}_1^0) = 24$. Therefore, the mapping π for these two spaces can not be surjective, which is another difference between a regular T-mesh and a nonregular T-mesh.

Fig. 15 Figures for Lemma 5.3

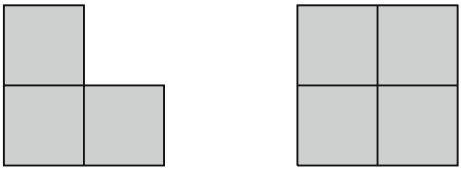

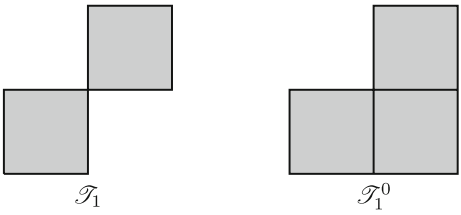

Fig. 16 Extend functions of spline space over nonregular T-mesh

Theorem 5.4 *For a regular T-mesh $\mathscr{T}$, suppose the holes of $\mathscr{T}$ are all rectangles. Using the previously introduced symbols, for $\mathscr{T}^s$, if no T-junctions exist on the edges of the cell C_i^0 $(1 \leqslant i \leqslant H)$ (refer to $\mathscr{T}_1$ in Figure 14 for an example), then*

$$\dim \mathbf{S}_d(\mathscr{T}) = \dim \mathbf{S}_d(\mathscr{T}^s)$$

Proof We prove this lemma for $H = 1$. The proof confirms that the number of holes does not affect the conclusion.

We should prove that the mapping π in Lemma 5.2 is surjective. For any $f \in \mathbf{S}_d(\mathscr{T})$, if f' is its extension on $\Omega(\mathscr{T}^s)$, then the B-coefficients of f' corresponding to the domain points of $\mathscr{T}$ are the same as that of f. To verify whether f' exists, we verify whether we can obtain a sequence of B-coefficients defined on C_1^0 that satisfy the smoothness conditions.

By the B-net method, only the functions defined on the four cells adjacent to C_1^0 will affect the B-coefficients corresponding to the domain points of C_1^0. Because $\mathscr{T}$ is regular, we can prove this theorem based on Fig. 17, which pertains to the special case $d = 3$. The $(d+1)^2$ B-coefficients are determined by the C^{d-1} continuous condition and every B-coefficient is determined more than once. We verify that the B-coefficients corresponding to the same domain point determined by different functions are equivalent.

Suppose the $(d+1)^2$ B-coefficients are $c_{i,j}, 0 \leqslant i \leqslant d, 0 \leqslant j \leqslant d$, which are ordered as in Section 3.1. The common B-coefficients that are determined by

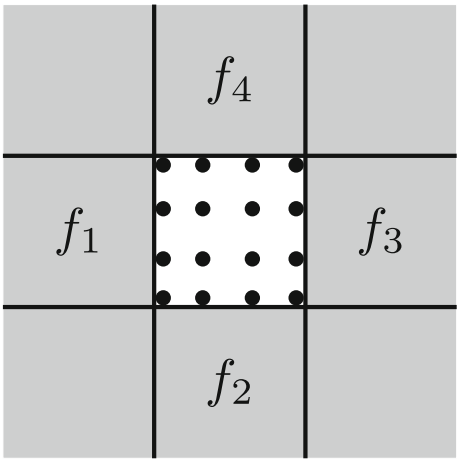

Fig. 17 Figure for Theorem 5.4. ($d = 3$)

f_1 and f_2 are $c_{i,j}, 0 \leqslant i \leqslant d-1, 0 \leqslant j \leqslant d-1$. By Lemma 5.3, we know that the d^2 B-coefficients determined by f_1 are the same as that determined by f_2 correspondingly. Similarly, we obtain the same conclusions on f_2 and f_3, f_3 and f_4, and f_4 and f_1. For f_2 and f_4, the common B-coefficients determined by the two functions are $c_{i,j}, 0 \leqslant i \leqslant d, j = 1, 2, \ldots, d-1$. The B-coefficients $c_{i,j}, 0 \leqslant i \leqslant d-1, j = 1, 2, \ldots, d-1$ determined by f_2 and f_4 are both the same as that determined by f_1, and $c_{i,j}, 1 \leqslant i \leqslant d, j = 1, 2, \ldots, d-1$ determined by f_2 and f_4 are both the same as that determined by f_3. Therefore, the $(d+1)(d-1)$ B-coefficients determined by f_2 are the same as that determined by f_4 correspondingly. We have the same conclusions on f_1 and f_3.

Therefore, the mapping π is surjective. Combining with the conclusion that π is injective in Lemma 5.2, we prove this theorem. □

However, if T-junctions exist on the edges of C_1^0, this conclusion is not usually accurate. For example, for the T-mesh $\mathscr{T}$ in Fig. 13, $\dim \mathbf{S}_3(\mathscr{T}^s) = 38$, regardless of $x_1 = x_2$, which is not equal to $\dim \mathbf{S}_3(\mathscr{T})$. From the viewpoint of the B-net method, the extension of a spline function is to determine the B-coefficients of a piecewise function defined on Ω_1 (the region occupied by the cell C_1^0) under the C^{d-1} continuous condition. If the region Ω_1 is divided into additional cells, additional B-coefficients will exist, which indicates greater possibilities for extending spline spaces. Therefore, $\mathscr{T}^s$ is too coarse for the extension of $\mathbf{S}_d(\mathscr{T})$.

5.1 Surjective meshes

Definition 5.5 Given a simply connected quasi-TP mesh $\mathscr{T}$, let a TP mesh $\mathscr{T}_1$ be a submesh of $\mathscr{T}$. If there does not exist a TP mesh $\mathscr{T}_1'$, which is a submesh of $\mathscr{T}$, such that $\mathscr{T}_1$ is a nontrivial submesh of $\mathscr{T}_1'$, then $\mathscr{T}_1$ is called a **maximal TP mesh** contained in $\mathscr{T}$. If an L-edge of $\mathscr{T}_1$ is on an L-edge l of $\mathscr{T}$, we say l **crosses** $\mathscr{T}_1$.

For two maximal TP meshes $\mathscr{T}_1$ and $\mathscr{T}_2$, if there is at least a pair of adjacent cells c_1 and c_2 in $\mathscr{T}_1$ and $\mathscr{T}_2$, respectively, then we say $\mathscr{T}_1$ and $\mathscr{T}_2$ are **adjacent**.

In Fig. 18, the mesh $\mathscr{T}$ has four maximal TP meshes: $\mathscr{T}_1$, $\mathscr{T}_2$, $\mathscr{T}_3$ and $\mathscr{T}_4$. Each pair of $\mathscr{T}_1$, $\mathscr{T}_2$, $\mathscr{T}_3$ and $\mathscr{T}_4$ are adjacent. Four vertical L-edges cross $\mathscr{T}_1$: the L-edge between v_1 and v_3, the L-edge between v_4 and v_5, the L-edge between v_{15} and v_{16}, and the L-edge between v_6 and v_7.

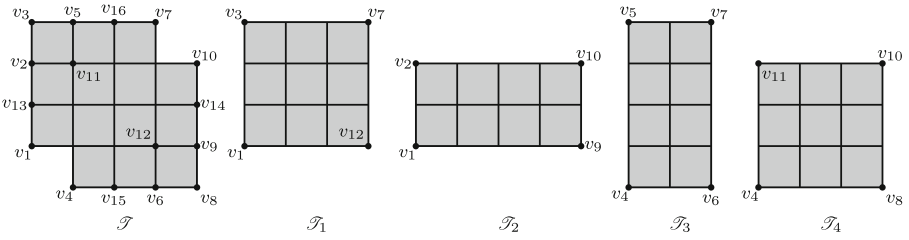

Fig. 18 Maximal TP meshes

For a quasi-TP mesh $\mathscr{T}$, the maximal TP meshes contained in $\mathscr{T}$ are $\mathscr{T}_1, \mathscr{T}_2, \ldots, \mathscr{T}_n$. If there is a subset $\{i_1, i_2, \ldots, i_k\}$ of $\{1, 2, \ldots, n\}$, such that

$$\bigcup_{j=1}^{k} \Omega(\mathscr{T}_{i_j}) = \Omega(\mathscr{T}), \tag{6}$$

and for any nontrivial subset of $\{i_1, i_2, \ldots, i_k\}$, Equation (6) does not hold. Then, we say $\mathscr{T}$ can be **divided** into $\mathscr{T}_{i_1}, \ldots, \mathscr{T}_{i_k}$, which is denoted by $\mathscr{T} = \biguplus_{j=1}^{k} \mathscr{T}_{i_j}$. Without considering the ordering, the division of a quasi-TP mesh is unique. For the quasi-TP mesh $\mathscr{T}$ in Fig. 18, $\mathscr{T} = \mathscr{T}_1 \uplus \mathscr{T}_4$.

Definition 5.6 Suppose $\mathscr{T}$ is a simply connected quasi-TP mesh and $\mathscr{T} = \mathscr{T}_1 \uplus \mathscr{T}_2 \uplus \cdots \uplus \mathscr{T}_m$. If $\mathscr{T}_k$ $(1 \leqslant k \leqslant m)$ has at least $d+1$ vertical L-edges and $d+1$ horizontal L-edges, and there are at least $d+1$ horizontal L-edges or $d+1$ vertical L-edges that cross both $\mathscr{T}_i$ and $\mathscr{T}_j$ when $\mathscr{T}_i$ and $\mathscr{T}_j$ are adjacent, then $\mathscr{T}$ is called a **surjective mesh**.

For the three quasi-TP meshes in Fig. 19, if $d = 2$, then the three meshes are surjective meshes; if $d = 3$, then $\mathscr{T}_1$ and $\mathscr{T}_3$ are surjective meshes, and $\mathscr{T}_2$ is not a surjective mesh.

If $\mathscr{T}$ is a surjective mesh, we want to compute $\dim \overline{\mathbf{S}}_d(\mathscr{T})$. By Lemma 4.4, we should only compute $\dim W[\mathscr{L}(\mathscr{T})]$. First we provide a lemma that is similar to Lemma 8.3 in [20].

Lemma 5.7 *Given a T-mesh $\mathscr{T}$, suppose there are $d+1$ horizontal L-edges $l_0^h, l_1^h, \ldots, l_d^h$ which are on $d+1$ different lines. Let $L = \{l_0^h, l_1^h, \ldots, l_d^h\}$, $\mathscr{L}(\mathscr{T})$ be the set of all L-edges of $\mathscr{T}$ and $\mathscr{L}(\mathscr{T})\backslash L$ be the complementary set of L in $\mathscr{L}(\mathscr{T})$. Then,*

$$\dim W[\mathscr{L}(\mathscr{T})] = \dim W[\mathscr{L}(\mathscr{T})\backslash L].$$

Proof Suppose all vertical L-edges are $l_0^v, l_1^v, l_2^v, \ldots, l_M^v$, the x-coordinates of which are $x_0, x_1, x_2, \ldots, x_M$, respectively, and all horizontal L-edges are $l_0^h, l_1^h, l_2^h, \ldots, l_N^h$, the y-coordinates of which are $y_0, y_1, y_2, \ldots, y_N$, respectively. Since $l_0^h, l_1^h, \ldots, l_d^h$ are on $d+1$ different lines, we have $y_i \neq y_j$ when $i \neq j, 0 \leqslant i, j \leqslant d$. We only

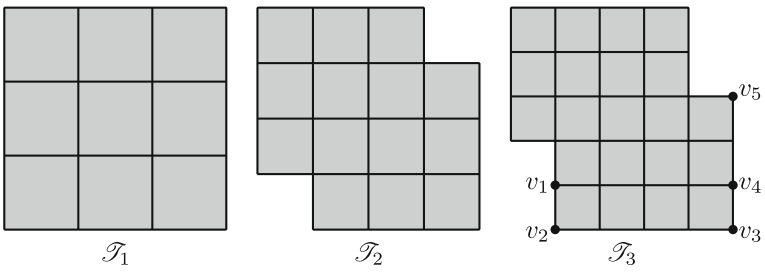

Fig. 19 Three quasi-TP meshes

need to prove that when $\mathscr{S}_{l_j^h} = 0$ for $j = d+1, d+2, \ldots, N$ and $\mathscr{S}_{l_j^v} = 0$ for $j = 0, 1, \ldots, M$, we have $\mathscr{S}_{l_j^h} = 0$ for $j = 0, 1, \ldots, d$.

For a vertical L-edge l_i^v, we use $v \in l_i^v$ to denote that v is a vertex on l_i^v. We have $\sum_{v \in l_i^v} c(v)(y - y(v))^d = 0$, where $c(v)$ is the vertex cofactor of v and $y(v)$ is the y-coordinate of v. Multiplying $(x - x_i)^d$, we have $(\sum_{v \in l_i^v} c(v)(y - y(v))^d)(x - x_i)^d = 0$. Therefore,

$$\begin{aligned} 0 &= \sum_{i=0}^{M} \Big(\sum_{v \in l_i^v} c(v)(y - y(v))^d\Big)(x - x_i)^d \\ &= \sum_{j=0}^{N} \Big(\sum_{v \in l_j^h} c(v)(x - x(v))^d\Big)(y - y_j)^d \\ &= \sum_{j=0}^{d} \Big(\sum_{v \in l_j^h} c(v)(x - x(v))^d\Big)(y - y_j)^d \end{aligned}$$

The last equation holds because $\mathscr{S}_{l_j^h} = 0$ for $j = d+1, d+2, \ldots, N$. Because $(y - y_j)^d$, $j = 0, 1, \ldots, d$ form a basis of $\mathbb{P}_d[y]$, we obtain $\mathscr{S}_{l_j^h} = 0$ for $j = 0, 1, \ldots, d$, which proves the lemma. □

Lemma 5.8 *Given a surjective mesh $\mathscr{T}$ with V vertices and E L-edges, it follows that*

$$\dim \overline{\mathbf{S}}_d(\mathscr{T}) = V - (d+1)E + (d+1)^2.$$

Proof Suppose $\mathscr{T} = \mathscr{T}_1 \uplus \mathscr{T}_2 \uplus \cdots \uplus \mathscr{T}_m$. The submesh $\mathscr{T}_1$ has at least $d+1$ horizontal L-edges. We assume that $d+1$ of these L-edges are on $d+1$ L-edges $l_0, l_1, \ldots, l_d$ of $\mathscr{T}$. We use $\mathscr{L}(\mathscr{T})$ and L to denote the set of all L-edges of $\mathscr{T}$ and the set $\{l_0, l_1, \ldots, l_d\}$, respectively. By Lemma 5.7, we have

$$\dim \overline{\mathbf{S}}_d(\mathscr{T}) = \dim W[\mathscr{L}(\mathscr{T})] = \dim W[\mathscr{L}(\mathscr{T}) \backslash L].$$

We prove that $\mathscr{L}(\mathscr{T}) \backslash L$ has a reasonable ordering. First, assume that $m = 2$. Because $\mathscr{T}$ is a surjective mesh, without losing generality, we assume that there are at least $d+1$ vertical L-edges that cross both $\mathscr{T}_1$ and $\mathscr{T}_2$. Suppose the L-edges of $\mathscr{T}$ that cross $\mathscr{T}_2$ but not cross $\mathscr{T}_1$ are $l_{2,1}^h, \ldots, l_{2,r}^h, l_{2,1}^v, \ldots, l_{2,s}^v$, where $l_{2,i}^h$ and $l_{2,j}^v$ are horizontal L-edges and vertical L-edges, respectively. For example, for the T-mesh $\mathscr{T}_3$ in Fig. 19, $r = 2, s = 1$ and $l_{2,1}^h, l_{2,2}^h, l_{2,1}^v$ are the L-edges between v_1 and v_4, v_2 and v_3, v_3 and v_5, respectively. Because $\mathscr{T}_2$ has at least $d+1$ vertical L-edges and $d+1$ horizontal L-edges and at least $d+1$ vertical L-edges cross both $\mathscr{T}_1$ and $\mathscr{T}_2$, $l_{2,1}^v, \ldots, l_{2,s}^v, l_{2,1}^h, \ldots, l_{2,r}^h$ is a reasonable ordering. Suppose the L-edges not including the elements in L that cross $\mathscr{T}_1$ are $l_{1,1}^h, \ldots, l_{1,r'}^h, l_{1,1}^v, \ldots, l_{1,s'}^v$. Because $\mathscr{T}_1$ has at least $d+1$ vertical L-edges and $d+1$ horizontal L-edges, $l_{2,1}^v, \ldots, l_{2,s}^v, l_{2,1}^h, \ldots, l_{2,r}^h, l_{1,1}^h, \ldots, l_{1,r'}^h, l_{1,1}^v, \ldots, l_{1,s'}^v$ is a reasonable ordering of

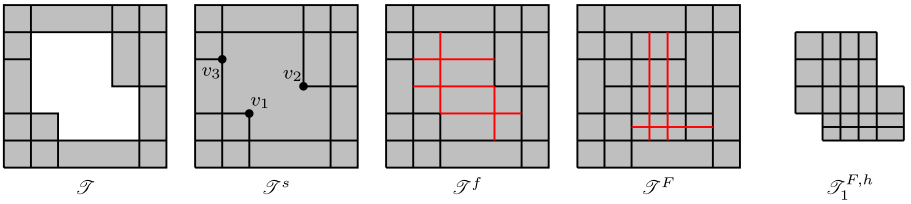

Fig. 20 Generate a filled mesh. ($d = 3$)

$\mathscr{L}(\mathscr{T})\backslash L$. By induction, we know that $\mathscr{L}(\mathscr{T})\backslash L$ has a reasonable ordering for any m. Therefore,

$$\dim W[\mathscr{L}(\mathscr{T})\backslash L] = V - (d+1)(E - (d+1)) = V - (d+1)E + (d+1)^2,$$

which completes the proof. □

5.2 Filled meshes

Definition 5.9 Suppose $\mathscr{T}$ is a T-mesh with H holes. The regions occupied by these holes are $\Omega_1, \Omega_2, \ldots, \Omega_H$. If there are H surjective meshes $\mathscr{T}_1^{F,h}, \mathscr{T}_2^{F,h}, \ldots, \mathscr{T}_H^{F,h}$, such that $\Omega(\mathscr{T}_i^{F,h}) = \Omega_i$, and the T-junctions on the boundary of Ω_i in $\mathscr{T}^s$ become crossing-vertices (the interior vertices of valence four) in the simply connected T-mesh $\mathscr{T}^F := \mathscr{T} \cup \mathscr{T}_1^{F,h} \cup \mathscr{T}_2^{F,h} \cdots \cup \mathscr{T}_H^{F,h}$, where $i = 1, 2, \ldots, H$, then $\mathscr{T}^F$ is called a **filled mesh** of $\mathscr{T}$.

For a T-mesh $\mathscr{T}$ with holes, the simply connected mesh $\mathscr{T}^s$ corresponding to it may be not a T-mesh. There is a new type of vertex in $\mathscr{T}^s$ - L-vertex, which is the end points of two c-edges. For the T-mesh $\mathscr{T}$ in Fig. 20, v_1 and v_2 are L-vertices. We generate a filled mesh $\mathscr{T}^F$ in the following manner: For the edges with an end point, which is a T-junction or an L-vertex on the boundary of Ω_1, we extend the edges to reach the boundary of Ω_1. The resulting mesh is $\mathscr{T}^f$; the mesh defined on Ω_1 is $\mathscr{T}_1^h$; and the red line segments are the added edges. Then, we add some line segments to change $\mathscr{T}_1^h$ into a surjective mesh. The resulting mesh is $\mathscr{T}^F$; the surjective mesh defined on Ω_1 is $\mathscr{T}_1^{F,h}$; and the red line segments are the added edges.

For a surjective mesh $\mathscr{T}$, we use $D(\mathscr{T})$ to denote the outermost d layers of the domain points. In Fig. 21, $D(\mathscr{T}_1)$ and $D(\mathscr{T}_3)$ are denoted by "•" for the two meshes in Fig. 19. Because a surjective mesh is a quasi-TP mesh, we label the outermost domain points of a cell on the edges for convenience.

Fig. 21 The outermost d layers of domain points

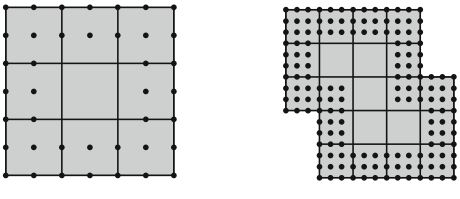

$D(\mathscr{T}_1)$ ($d = 2$) $D(\mathscr{T}_3)$ ($d = 3$)

For a T-mesh $\mathscr{T}$ with H holes, a corresponding filled mesh is $\mathscr{T}^F$. We know that the B-coefficients corresponding to $D(\mathscr{T}_1^{F,h}), D(\mathscr{T}_2^{F,h}), \ldots, D(\mathscr{T}_H^{F,h})$ are determined by the functions around the holes. By the construction manner of the filled mesh and Lemma 5.3, we know that the B-coefficients corresponding to the same domain point determined by different functions are equivalent.

Lemma 5.10 *For a T-mesh $\mathscr{T}$ with H holes, a corresponding filled mesh is $\mathscr{T}^F$. For any function $g \in \mathbf{S}_d(\mathscr{T})$, we can obtain a series of B-coefficients corresponding to $D(\mathscr{T}_i^{F,h})$, which is determined by g, where $1 \leqslant i \leqslant H$. Then, the B-coefficients corresponding to $D(\mathscr{T}_i^{F,h})$ satisfy C^{d-1} continuous conditions among themselves. If we use B_i to denote the space of the B-coefficients corresponding to $D(\mathscr{T}_i^{F,h})$, we have*

$$\dim B_i \leqslant dV_i^b, \tag{7}$$

where V_i^b is the number of boundary vertices of $\mathscr{T}_i^{F,h}$.

Proof That the B-coefficients corresponding to $D(\mathscr{T}_i^{F,h})$ satisfy C^{d-1} continuous conditions among themselves is guaranteed by the C^{d-1} continuity of g. The verification is not very difficult. We omit the process here.

To prove Inequality (7), we need to prove that the number of elements of the determining set of $D(\mathscr{T}_i^{F,h})$ is not more than dV_i^b. We prove this conclusion for $D(\mathscr{T}_3)$ in Fig. 22. Since $\mathscr{T}_3$ is a surjective mesh, we can select the top-left cell (the cell in red) as the beginning cell and traverse all boundary cells in counter-clockwise direction. We denote the top-left vertex of the beginning cell as O_1. We construct a set of domain points D with some elements of $D(\mathscr{T}_3)$. For the beginning cell, the d^2 domain points labelled by "▲" are selected. For each vertex of the boundary vertices beginning at A and ending at B in counter-clockwise direction, the d domain points labelled by "•" are selected. Here A is the left-bottom vertex of the beginning cell and B is the $d+1$th vertex of the top L-edge from the left, which indicates that d vertices are not considered. In Fig. 22, the d vertices are O_1, O_2, O_3. The resulting

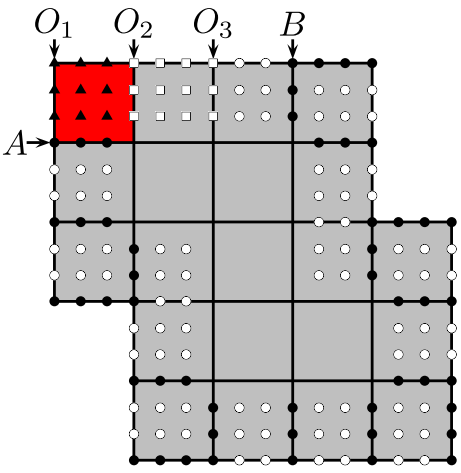

Fig. 22 The determining set of $D(\mathscr{T}_3)$. ($d = 3$)

set D consists of the domain points labelled by "▲" and "•". We claim that D is the determining set of $D(\mathscr{T}_3)$.

Suppose the B-coefficients corresponding to D are zeroes. By the C^{d-1} continuous condition, we can verify that the B-coefficients corresponding to the domain points labelled by "∘" are zeroes. For the domain points labelled by "□", we consider a univariate spline function $h(t)$ with degree d and C^{d-1} continuous defined on $d+1$ knots. See Fig. 23. The $d+1$ knots are $t_0, t_1, t_2, \ldots, t_d$. When the B-coefficients corresponding to the domain points labelled by "▲" and "•" are zeros, the function $h(t)$ is zero when $t < t_0$ or $t > t_d$. Since the support of a nonzero spline function with degree d should have at least $d+2$ breakpoints, we obtain $h(t) \equiv 0$, which indicates that the B-coefficients corresponding to the domain points labelled by "□" are zeroes. For the $d(d(d-2)+1)$ domain points labelled by "□" in Fig. 22, using the conclusion for a univariate spline function d times, we obtain that the B-coefficients corresponding to them are zeroes. Therefore,

$$\dim B_i \leqslant \#D = d^2 + d(V^b - d) = dV^b,$$

where $\#D$ is the number of elements of D and V^b is the number of boundary vertices of $\mathscr{T}_3$.

All surjective meshes have a similar structure. The conclusions can be similarly obtained. □

For a T-mesh $\mathscr{T}$ with holes, $\mathscr{T}^F$ is its filled mesh. Consider the following mapping:

$$\begin{aligned} \pi: \quad \mathbf{S}_d(\mathscr{T}^F) &\longrightarrow \mathbf{S}_d(\mathscr{T}) \\ f &\longmapsto f|_{\Omega(\mathscr{T})}. \end{aligned} \tag{8}$$

With the symbols in Lemma 5.10, for a hole Ω_1, that the mapping π is surjective indicates that, for any series of B-coefficients in B_i, we can obtain a series of B-coefficients corresponding to the domain points of $\mathbf{S}_d(\mathscr{T}_1^{F,h})$ except the domain points in $D(\mathscr{T}_1^{F,h})$. That is, the projection mapping

$$\pi': \quad B(\mathbf{S}_d(\mathscr{T}_1^{F,h})) \longrightarrow B_1 \tag{9}$$

is surjective, where $B(\mathbf{S}_d(\mathscr{T}_1^{F,h}))$ is the space of the B-coefficients corresponding to all domain points of $\mathbf{S}_d(\mathscr{T}_1^{F,h})$.

Lemma 5.11 *For a T-mesh $\mathscr{T}$ with H holes, $\mathscr{T}^F$ is its filled mesh. If $\dim \overline{\mathbf{S}}_d(\mathscr{T}_i^{F,h}) = V_i - (d+1)E_i + (d+1)^2$, where $1 \leqslant i \leqslant H$ and V_i, E_i are the numbers of vertices and L-edges of $\mathscr{T}_i^{F,h}$, respectively, then the mapping π in Equation (8) is surjective.*

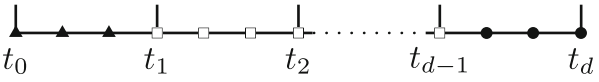

Fig. 23 The determining set for a univariate spline function

Proof We only need to prove that the mapping π' in Equation (9) is surjective. By Lemma 4.5, we have $\dim B(\mathbf{S}_d(\mathscr{T}_1^{F,h})) = \dim \mathbf{S}_d(\mathscr{T}_1^{F,h}) = V_1 + dV_1^b - (d+1)E_1 + (d+1)^2$, where V_1^b is the number of boundary vertices of $\mathscr{T}_1^{F,h}$. It is apparent that $\operatorname{Ker}\pi' = B(\overline{\mathbf{S}}_d(\mathscr{T}_1^{F,h}))$. Therefore, $\dim \operatorname{Ker}\pi' = \dim \overline{\mathbf{S}}_d(\mathscr{T}_1^{F,h}) = V_1 - (d+1)E_1 + (d+1)^2$. By Inequality (7), it follows that

$$\begin{aligned} V_1 + dV_1^b - (d+1)E_1 + (d+1)^2 = \dim B(\mathbf{S}_d(\mathscr{T}_1^{F,h})) &= \dim \operatorname{Ker}\pi' + \dim \operatorname{Im}\pi' \\ &\leqslant \dim \operatorname{Ker}\pi' + \dim B_1 \\ &\leqslant V_1 + dV_1^b - (d+1)E_1 + (d+1)^2. \end{aligned}$$

Therefore, $\dim \operatorname{Im}\pi' = \dim B_1$, which indicates that the mapping π is surjective. We complete the proof. □

Theorem 5.12 *For a regular T-mesh $\mathscr{T}$ with H holes, $\mathscr{T}^F$ is its filled mesh and $\mathscr{T}_1^{F,h}, \mathscr{T}_2^{F,h}, \ldots, \mathscr{T}_H^{F,h}$ are the H surjective meshes defined on $\Omega_1, \Omega_2, \ldots, \Omega_H$. Then*

$$\dim \mathbf{S}_d(\mathscr{T}) = \dim \mathbf{S}_d(\mathscr{T}^F) - \sum_{i=1}^{H} \dim \overline{\mathbf{S}}_d(\mathscr{T}_i^{F,h}).$$

Proof We construct the mapping

$$\begin{aligned} \pi: \quad \mathbf{S}_d(\mathscr{T}^F) &\longrightarrow \mathbf{S}_d(\mathscr{T}) \\ f &\longmapsto f|_{\Omega(\mathscr{T})}. \end{aligned}$$

By Lemma 5.11 and Lemma 5.8, we know that π is surjective.

For any function $f \in \operatorname{Ker}\pi$, f is zero out of $\Omega_1, \Omega_2, \ldots, \Omega_H$. Since $\mathscr{T}$ is regular, the domain Ω_i does not intersect Ω_j, $i \neq j$. Therefore, $\operatorname{Ker}\pi = \overline{\mathbf{S}}_d(\mathscr{T}_1^{F,h}) \oplus \overline{\mathbf{S}}_d(\mathscr{T}_2^{F,h}) \oplus \cdots \overline{\mathbf{S}}_d(\mathscr{T}_H^{F,h})$, which indicates $\dim \operatorname{Ker}\pi = \sum_{i=1}^{H} \dim \overline{\mathbf{S}}_d(\mathscr{T}_i^{F,h})$.

Because $\dim \mathbf{S}_d(\mathscr{T}^F) = \dim \operatorname{Im}\pi + \dim \operatorname{Ker}\pi = \dim \mathbf{S}_d(\mathscr{T}) + \dim \operatorname{Ker}\pi$, the conclusion is correct. □

Combining Lemma 4.2, Lemma 5.8 and Theorem 5.12, we obtain the following corollary.

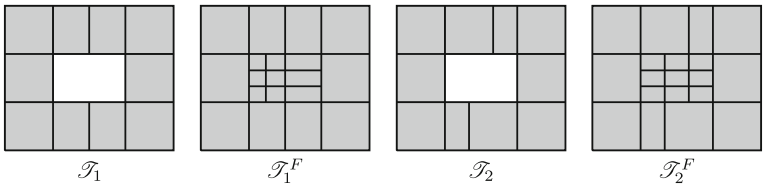

Fig. 24 Figures for Example 5.14

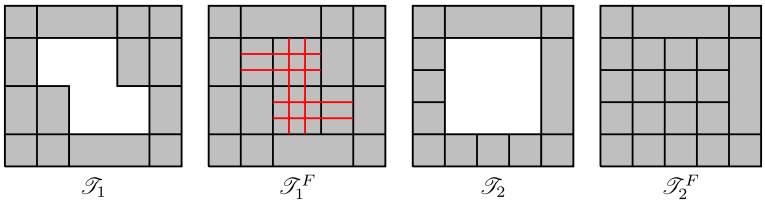

Fig. 25 Figures for Example 5.16

Corollary 5.13 *For a regular T-mesh $\mathscr{T}$ with H holes, $\mathscr{T}^F$ is its filled mesh and $\mathscr{T}_i^{F,h}$ is the surjective mesh defined on Ω_i, $1 \leqslant i \leqslant H$. Suppose $\mathscr{T}^F$ has G_F cross-cuts, V_F^i interior vertices, M_F is the conformality matrix of all of the T c-edges of $\mathscr{T}^F$, and suppose $\mathscr{T}_i^{F,h}$ has V_i vertices, E_i L-edges. Then*

$$\dim \mathbf{S}_d(\mathscr{T}) = V_F^i + (d+1)G_F - \operatorname{rank} M_F - \sum_{i=1}^{H} V_i + (d+1)\sum_{i=1}^{H} E_i - (H-1)(d+1)^2.$$

Example 5.14 We consider the mesh in Fig. 13. The two situations are illustrated in Fig. 24. When $x_1 = x_2$, the mesh is $\mathscr{T}_1$; otherwise, the mesh is $\mathscr{T}_2$.

By Corollary 5.13, we obtain $\dim \mathbf{S}_3(\mathscr{T}_1) = 42$, $\dim \mathbf{S}_3(\mathscr{T}_2) = 40$.

Example 5.15 We consider the mesh in Fig. 20. By Corollary 5.13, we obtain $\dim \mathbf{S}_3(\mathscr{T}) = 54$.

Sometimes, although the simply connected mesh $\mathscr{T}^s$ corresponding to $\mathscr{T}$ is not very complex, computing $\dim \mathbf{S}_d(\mathscr{T}^F)$ is not very easy, and $\dim \overline{\mathbf{S}}_d(\mathscr{T}_i^{F,h})$ may be nonzero. We consider two examples.

Example 5.16 We consider the two meshes in Fig. 25.

By Lemma 5.8, $\dim \overline{\mathbf{S}}_3(\mathscr{T}_{1,1}^{F,h}) = 0$, $\dim \overline{\mathbf{S}}_2(\mathscr{T}_{2,1}^{F,h}) = 1$. By Lemma 4.2, we obtain $\dim \mathbf{S}_2(\mathscr{T}_2^F) = 37$. To compute $\dim \mathbf{S}_3(\mathscr{T}_1^F)$, we should compute $\dim W[\mathscr{C}(\mathscr{T}_1)]$, where $\mathscr{C}(\mathscr{T}_1)$ is the set of all T c-edges of $\mathscr{T}_1$ (represented by red line segments). This problem has been discussed in Lemma 6.12 in [32]; the conclusion is $\dim W[\mathscr{C}(\mathscr{T}_1)] = 2$. By Equation (5), we obtain $\dim \mathbf{S}_3(\mathscr{T}_2^F) = 48 + 2 = 50$. Therefore, we have $\dim \mathbf{S}_3(\mathscr{T}_1) = 50$ and $\dim \mathbf{S}_2(\mathscr{T}_2) = 37 - 1 = 36$.

6 Conclusions and future studies

We mainly explore the dimensions of spline spaces over non-rectangular T-meshes in this paper. The dimension formulae of the spline spaces over simply connected hierarchical T-meshes have been obtained. To explore the dimension problem of spline spaces over T-meshes with holes, we discover a new type of instability of the dimensions. We construct the relationship between the dimension of the spline space over

a T-mesh with holes and the dimension of the spline space over over a simply connected mesh, which is suitable for the extension of spline functions. We provide several examples for the dimension computation.

The construction a basis for the spline space over a non-rectangular T-mesh is a considerable problem for future research.

Acknowledgments The authors are supported by a NKBRPC (2011CB302400), the NSF of China (11031007 ,11371341 and 11526069), the 111 Project (No. b07033), the Anhui Provincial Natural Science Foundation (No. 1608085QA14), and the Open Project Program of the State Key Lab of CAD&CG (A1601) , Zhejiang University.

References

1. Berdinsky, D., Oh, M., Kim, T., Mourrain, B.: On the problem of instability in the dimension of a spline space over a T-mesh. Comput. Graph. **36**(5), 507–513 (2012)
2. Chui, C., Lai, M.: Filling polygonal holes using C^1 cubic triangular spline patches. Comput. Aided Geom. Des. **17**, 297–307 (2000)
3. Cohen, E., Martin, T., Kirby, R.M., Lyche, T., Riesenfeld, R.F.: Analysis-aware modeling: understanding quality considerations in modeling for isogeometric analysis. Comput. Methods Appl. Mech. Eng. **199**, 334–356 (2010)
4. Deng, J., Chen, F., Feng, Y.: Dimensions of spline spaces over T-meshes. J. Comput. Appl. Math. **194**, 267–283 (2006)
5. Deng, J., Chen, F., Li, X., Hu, C., Tong, W., Yang, Z., Feng, Y.: Polynomial splines over hierarchical T-meshes. Graph. Model. **74**, 76–86 (2008)
6. Deng, J., Chen, F., Jin, L.: Dimensions of biquadratic spline spaces over T-meshes. J. Comput. Appl. Math. **238**, 68–94 (2013)
7. Diener, D.: Instability in the dimension of spaces of bivariate piecewise polynomials of degree $2r$ and smoothness order r. SIAM J. Numer. Anal. **27**, 543–551 (1990)
8. Fortes, M., González, P., Pasadas, M., Rodríguez, M.: Hole filling on surfaces by discrete variational splines. Appl. Numer. Math. **62**, 1050–1060 (2012)
9. Giannelli, C., Jüttler, B., Speleers, H.: Strongly stable bases for adaptively refined multilevel spline spaces. Adv. Comput. Math. **40**(2), 459–490 (2014)
10. Gregory, J., Lau, V., Zhou, J.: Smooth parametric surfaces and N-Sided patches. In: Computation of Curves and Surfaces, pp. 457-498. Springer, Netherlands (1990)
11. Gregory, J., Zhou, J.: Filling polygonal holes with bicubic patches. Comput. Aided Geom. Des. **11**, 391–410 (1994)
12. Huang, Z., Deng, J., Li, X.: Dimensions of spline spaces over general T-meshes. J. Univ. Sci. Technol. China **36**(6), 573–581 (2006)
13. Huang, Z., Deng, J., Feng, Y., Chen, F.: New proof of dimension formula of spline spaces over t-meshes via smoothing cofactors. J. Comput. Math. **24**, 501–514 (2006)
14. Hughes, T.J.R., Cottrell, J.A., Bazilevs, Y.: Isogeometric analysis: CAD, finite elements, NURBS, exact geometry and mesh refinement. Comput. Methods Appl. Mech. Eng. **194**, 4135–4195 (2005)
15. Karciauskas, K., Peters, J.: Smooth multi-sided blending of biquadratic splines. Comput. Graph. **46**, 172–185 (2015)
16. Li, C.J., Wang, R.H., Zhang, F.: Improvement on the dimensions of spline spaces on T-Mesh. J. Inf. Comput. Sci. **3**(2), 235–244 (2006)
17. Li, X., Deng, J., Chen, F.: Polynomial splines over general T-meshes. Vis. Comput. **26**, 277–286 (2010)
18. Li, X., Chen, F.: On the instability in the dimension of spline space over particular T-meshes. Comput. Aided Geom. Des. **28**, 420–426 (2011)
19. Li, X., Deng, J.: On the dimension of spline spaces over T-meshes with smoothing cofactor-conforMality method. Comput. Aided Geom. Des. **41**, 76–86 (2016)

20. Li, X., Scott, M.A.: Analysis-suitable T-splines: characterization, refieability, and approximation. Math. Models Methods Appl. Sci. **24**(06), 1141–1164 (2014)
21. Morgan, J., Scott, R.: The dimension of C^1 piecewise polynomials. Unpublished Manuscript (1977)
22. Mourrain, B.: On the dimension of spline spaces on planar T-meshes. Math. Comput. **83**(286), 847–871 (2014)
23. Navau, J., Garcia, N.: Modeling surfaces from meshes of arbitrary topology. Comput. Aided Geom. Des. **17**, 643–671 (2000)
24. Schumaker, L.L., Schempp, W., Zeller, K.: On the dimension of spaces of piecewise polynomials in two variables. In: Multivariate Approximation Theory, pp. 396-412. Birkhauser Verlag, Basel (1979)
25. Lai, M.J., Schumaker, L.L.: Spline Functions on Triangulations. Cambridge University Press, Cambridge (2007)
26. Schumaker, L.L., Wang, L.: Spline spaces on TR-meshes with hanging vertices. Numer. Math. **118**, 531–548 (2011)
27. Schumaker, L.L., Wang, L.: Approximation power of polynomial splines on T-meshes. Comput. Aided Geom. Des. **29**, 599–612 (2012)
28. Wu, M., Deng, J., Chen, F.: Dimension of spline spaces with highest order smoothness over hierarchical T-meshes. Comput. Aided Geom. Des. **30**, 20–34 (2013)
29. Wang, R.H.: Multivariate spline functions and their applications. Science Press/Kluwer Academic Publishers (2001)
30. Xu, G., Mourrain, B., Duvigneau, R., Galligo, A.: Parameterization of computational domain in isogeometric analysis: methods and comparison. Comput. Methods Appl. Mech. Eng. **200**, 2021–2031 (2011)
31. Xu, J., Chen, F., Deng, J.: Two-dimensional domain decomposition based on skeleton computation for parameterization and isogeometric analysis. Comput. Methods Appl. Mech. Eng. **284**, 541–555 (2015)
32. Zeng, C., Deng, F., Li, X., Deng, J.: Dimensions of biquadratic and bicubic spline spaces over hierarchical T-meshes. J. Comput. Appl. Math. **287**, 162–178 (2015)